JGR Earth Surface

RESEARCH ARTICLE
10.1029/2020JF006011

Key Points:

- We measured floodplain large wood and organic matter jams deposited after a large flood in the Colorado Front Range, USA
- River corridor morphology and forest stand density influence the amount and frequency of large wood and organic matter jams
- Reaches with steeper slopes had smaller jam loads and reaches with higher forest stand density had more organic matter jams

Supporting Information:

Supporting Information may be found in the online version of this article.

Correspondence to:

K. B. Lininger,
katherine.lininger@colorado.edu

Citation:

Lininger, K. B., Scamardo, J. E., & Guiney, M. R. (2021). Floodplain large wood and organic matter jam formation after a large flood: Investigating the influence of floodplain forest stand characteristics and river corridor morphology. *Journal of Geophysical Research: Earth Surface*, *126*, e2020JF006011. https://doi.org/10.1029/2020JF006011

Received 30 NOV 2020
Accepted 8 JUN 2021

Floodplain Large Wood and Organic Matter Jam Formation After a Large Flood: Investigating the Influence of Floodplain Forest Stand Characteristics and River Corridor Morphology

K. B. Lininger[1], J. E. Scamardo[2], and M. R. Guiney[1]

[1]Department of Geography, University of Colorado Boulder, Boulder, CO, USA, [2]Department of Geosciences, Colorado State University, Fort Collins, CO, USA

Abstract The controls on large wood (LW; wood >1 m in length and >0.1 m in diameter) and coarse particulate organic matter (CPOM; organic material >1 mm in diameter) deposition on floodplains have rarely been assessed, and there are few studies that explore the bidirectional interactions between wood, standing trees, and geomorphic processes. We use field data from West Creek, Colorado, USA, to assess the influence of river corridor morphology and forest stand density on the depositional patterns of floodplain LW and CPOM accumulations (jams) resulting from an extreme flood. Relatively high LW loads per area (mean ± SE = 678.6 ± 192.3 m^3 ha^{-1}) point to the importance of extreme floods for LW deposition on floodplains. We find that LW jams decreased in size with distance from and elevation above the channel, but that CPOM jams did not, demonstrating that the relatively smaller CPOM can be more easily transported within a forested floodplain. Steeper reaches contained smaller LW and CPOM loads per area, which may indicate that reaches with higher stream power during the flood were less depositional. As forest stand density increased, the number of CPOM jams per area increased, and a majority of jams were pinned by standing trees. Trees were trapping locations for LW and CPOM, highlighting the importance of preserving riparian forests. Floodplain LW and CPOM provide habitat and nutrients to floodplain ecosystems and influence geomorphic processes, creating an opportunity to use LW in restoration while reducing potential hazards caused by in-channel LW.

Plain Language Summary Downed, dead pieces of large wood, and organic matter influence physical and ecological processes in rivers and floodplains. Many river restoration efforts add wood into channels provide habitat for organisms, but wood on floodplains can also create habitat and provide ecosystem benefits. However, very little is known about how wood and organic matter are deposited on floodplains. We use field data from the Colorado Front Range to assess patterns of wood and organic matter deposition on floodplains resulting from an extreme flood, exploring the bidirectional interactions between wood, standing trees, and physical processes. We find that large wood accumulations decrease in size with distance from the river channel, but that organic matter accumulations do not, indicating that organic matter can be more easily moved further into the floodplain during a flood. Steeper portions of the river and floodplain had lower amounts of wood and organic matter, and trees were important trapping locations for accumulations during the flood. Our results point to the importance of preserving floodplain forests and inform the use of floodplain wood and organic matter in river restoration efforts.

1. Introduction

A large body of literature has demonstrated that wood in river corridors (which includes the channel, floodplain, and hyporheic zone (Harvey & Gooseff, 2015)) strongly influences geomorphic and ecological processes (e.g., Jones et al., 2014; Montgomery et al., 2003). However, processes of wood and organic matter transport, deposition, and storage on floodplains have received relatively little attention compared to wood and organic matter in channels (Lininger et al., 2017; Wohl, 2020), limiting our knowledge of floodplain geomorphic and hydraulic processes. In addition, although there has been substantial work looking at the interactions between living vegetation and geomorphic processes (e.g., Bywater-Reyes et al., 2017; Corenblit et al., 2009; Gurnell, 2014; Kui et al., 2014), there are relatively few studies that explore the bidirectional interactions between living vegetation, wood, and hydrogeomorphology (e.g., Bertoldi et al., 2015; Gurnell &

Petts, 2002). We assess the influence of geomorphic and forest stand characteristics in patterns of floodplain large wood (LW; >1 m in length and >0.1 m in diameter) and coarse particulate organic matter (CPOM; material >1 mm in diameter) deposition resulting from an extreme flood in the Colorado Rocky Mountains, USA.

In addition to informing ecogeomorphic dynamics in river corridors, determining controls on LW and CPOM deposition in floodplains supports river restoration and management efforts, since floodplain LW and CPOM support ecological processes and promote physical complexity. For example, buried floodplain LW accumulations (i.e., jams) can create hard points within floodplains, resisting erosion and promoting avulsion, and multithread planforms (Collins et al., 2012). Floodplain LW results in complex flow pathways during overbank flow events and causes spatially heterogeneous floodplain sedimentation and relatively high sedimentation rates (Jeffries et al., 2003). LW jams deposited in secondary channels promotes channel abandonment, sediment infilling, and floodplain formation and complexity (Montgomery & Abbe, 2006; Sear et al., 2010). Floodplain LW and CPOM also provide ecological functions, such as nutrient-rich sites for seedling establishment (Pettit & Naiman, 2006), habitat for diverse biota (Benke, 2011; Mac Nally et al., 2001), a large reservoir of organic carbon (Lininger et al., 2017), and enhancement of floodplain soil nutrients (Zalamea et al., 2007). CPOM within jams can reduce jam porosity by filling in spaces between LW, increasing the impacts of jams on hydraulics (Livers et al., 2020; Manners et al., 2007).

Floodplain LW loads (volumes per area or total volume) are likely highest in regions with relatively high primary productivity and relatively low decay rates. High productivity can result in denser forests and larger trees, increasing the source of LW, and low decay rate result in LW persistence (Lininger et al., 2017; Ricker et al., 2016; Wohl, 2020). LW and CPOM on floodplains can come from delivery via standing vegetation (autochthonous to the floodplain) or delivery via fluvial transport or hillslope mass movements (allochthonous to the floodplain) (Wohl, 2020). Floodplain LW loads have been correlated with standing vegetation type of the surrounding floodplains, emphasizing that in certain environments, much of the downed LW on floodplains is locally sourced as opposed to transported from upstream (Lininger et al., 2017; Wohl et al., 2011). Autochthonous delivery of LW via standing vegetation likely produces a pattern of individual LW pieces dispersed across the floodplain; in contrast, LW concentrated into jams indicates fluvial deposition and allochthonous delivery during flooding, since LW becomes concentrated and rearranged during transport and trapping. LW can also be incorporated into the floodplain after deposition in active secondary or side channels, becoming part of the floodplain surface or buried beneath the surface (e.g., Montgomery & Abbe, 2006; Wohl et al., 2018b).

Only a handful of studies investigate how hydrogeomorphic dynamics influence the amount and spatial distribution of LW jams deposited on floodplains (Galia et al., 2020; Pettit et al., 2005; Wohl et al., 2018a). Significant transport and deposition of LW can occur during large flood events (Comiti et al., 2016), but there has been very little work investigating the influence of flooding on patterns of floodplain LW deposition. In the semiarid mountainous western USA, drainages with high-magnitude disturbances such as frequent fires and high-magnitude floods tend to have a higher proportion of LW on the floodplain as opposed to within the channel, compared to drainages with low-magnitude disturbance (Wohl et al., 2018a). Large floods can uproot and deposit riparian vegetation in piles on floodplains and in valley bottoms (Pettit et al., 2005). Extreme flooding events can result in a significant source of wood due to debris flows, hillslope failures, and erosion of the floodplain and valley bottom (Steeb et al., 2017). Observations of wood in transport during flood events are uncommon, but extreme events can create hyper-congested wood-laden flows (Ruiz-Villanueva et al., 2016). Floods that transport significant amounts of wood have been shown to create large jams within channels, upstream of bridges, and on floodplain margins (Comiti et al., 2016; Steeb et al., 2017), but the dynamics of LW deposition onto floodplains has not been adequately explored.

River corridor geomorphology can also influence the amount and characteristics of LW deposition on floodplains. For example, the highest volumes of LW jams occurred in bedrock anastomosing channels on the Sabine River in South Africa compared to other channel types, due to the presence of trapping mechanisms such as bedrock outcrops and vegetation (Pettit et al., 2005). Wider valley bottoms can result in larger floodplain LW loads, potentially due to the dissipation of flood waters and subsequent LW deposition in unconfined portions of the river corridor (Pettit et al., 2005; Wohl et al., 2018a), but wider valley bottoms could also result in lower floodplain LW volumes if these reaches have dense forest vegetation, potentially

impeding transport (Galia et al., 2020). Measurements of CPOM jams have rarely been completed on floodplains, even though CPOM can be an important source of nutrients and can influences jam porosity (Livers et al., 2020; Manners et al., 2007).

In addition to hydrogeomorphic characteristics, vegetation also influences LW transport and deposition on floodplains. Floodplain trees can be an important source of LW during floods (Steeb et al., 2017; Zischg et al., 2018), and deposition of LW is likely influenced by the size and density of floodplain trees. Trees can serve as trapping locations on the floodplain and impede LW transport onto the floodplain surface, resulting in more deposition along the channel-floodplain boundary as opposed to the floodplain interior (Wohl, 2020). Previous work in the Pacific Northwest, USA found that LW jams incorporated into the floodplain provide hard points that resist erosion, promoting the growth of large riparian trees and a continued source of LW to the river channel (Collins et al., 2012). LW deposited within the river corridor can provide sites of seedling establishment and plant growth, stabilizing the surface and providing nutrients (Gurnell & Petts, 2002; Pettit & Naiman, 2006). Previous studies on the interaction between LW and vegetation have mainly focused on how LW influences subsequent vegetation growth and LW recruitment, but the influence of vegetation, such as riparian forest stand density, on LW and CPOM deposition onto floodplains has not been adequately studied.

Wood has been extensively used in river restoration efforts, but focus has mainly been on wood within the channel (Roni et al., 2015). Floodplain jams are likely more stable than jams in the channel (Lininger & Scott, 2019; Wohl et al., 2016), reducing hazards associated with the use of LW in restoration efforts. Thus, floodplain LW and CPOM jams can provide importance ecological benefits without the hazard associated with in-channel LW jams. However, quantitative data on how LW and CPOM loads vary both laterally across the floodplain and longitudinally along a river corridor are lacking, limiting knowledge on how to incorporate floodplain LW and CPOM into restoration efforts. Climate change predictions for the western USA include increased precipitation intensities or an increase in precipitation as rain when compared to snow, which could increase flood magnitudes and frequency (Davenport et al., 2020) and increase the amount of LW and CPOM deposited on floodplains. Understanding the dynamics of LW and CPOM deposition onto floodplains is important for both advancing understanding of LW and CPOM dynamics in river corridors and for river management and restoration efforts.

1.1. Objectives and Hypotheses

We use field data on floodplain LW and CPOM jams to assess the controls on jam deposition. Our field site is West Creek, located in the Colorado Front Range (CFR), USA, which experienced a 400-years flood event in 2013 (Yochum & Moore, 2013) and has significant amounts of LW and CPOM deposited on the floodplain. Because the flood on West Creek was extreme and resulted in widespread LW and CPOM deposition, it provided the opportunity to assess controls on floodplain LW and CPOM deposition across the entire floodplain and between reaches with varying geomorphic and forest stand characteristics. Our primary objective is to investigate the influences of both river corridor geomorphology and floodplain forest stand characteristics on the load and number (count) of floodplain LW and CPOM jams deposited by the flood.

The influence of river corridor morphology and floodplain forest stand characteristics can be explored through testing sets of hypotheses (Figure 1). If river corridor geomorphology influences floodplain jam formation and characteristics, we expect that there will be an inverse relationship between floodplain jam size and elevation above and distance from the bankfull channel (H1a). The floodplain jams were deposited during the 2013 flood event, and thus portions of the floodplain at higher elevation and greater distances relative to the channel likely experienced reduced transport capacity for LW and CPOM. Previous work has demonstrated that wood mobility is related to the ratio between wood diameter and flow depth (Braudrick & Grant, 2001; Dixon & Sear, 2014; Wohl & Goode, 2008); as flow depth on the floodplain decreased relative to wood diameter, we expect that wood mobility decreased and deposition occurred. Consequently, we expect that floodplain jam size will decrease with increasing elevation and distance from the channel because fewer pieces remained in transport. We also expect that floodplain LW jam counts and loads are higher in unconfined portions of the river corridor (H1b). Wider valley bottoms can cause flow attenuation during floods, dissipating, and temporarily storing flood waters (Lininger & Latrubesse, 2016; Woltemade & Potter, 1994). During the 2013 flood, confined reaches in the CFR tended to be locations with greater sediment

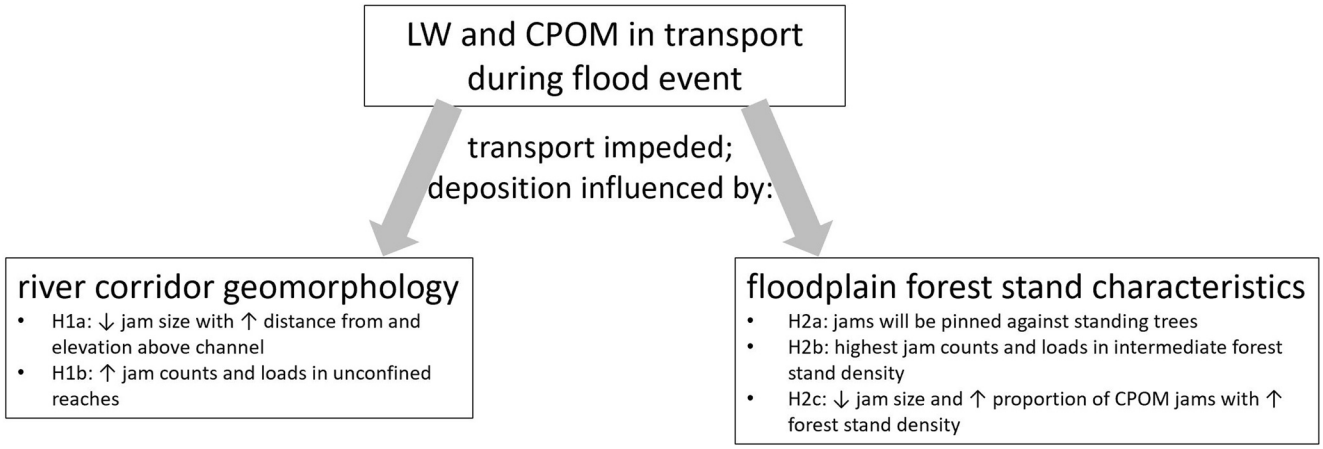

Figure 1. Conceptual diagram showing the expected influence of both river corridor geomorphology and floodplain forest stand characteristics on jam counts and jam loads of LW (large wood) and CPOM (coarse particulate organic matter).

erosion, while unconfined reaches experiences greater sediment deposition (Sholtes et al., 2018). Thus, we expect that unconfined portions of the river corridor promoted the deposition of jams onto the floodplain as opposed to continued transport of LW and CPOM downstream.

If floodplain forest stand density and characteristics influence floodplain jam deposition and characteristics, we expect that floodplain jams will be pinned against standing trees (H2a) as opposed to jams forming at other locations (e.g., bedrock outcrops or without a pinning mechanism). We also expect that there will be an intermediate floodplain forest stand density that promotes the highest floodplain jam loads and counts (H2b). If the floodplain forest is too dense, it would likely impede transport of wood onto the floodplain. However, if forest density is too low, a lack of trapping mechanisms would result in reduced jam loads and jam counts. We expect that dense floodplain forest stands will correlate with smaller average jam sizes and a greater proportion of CPOM jams as opposed to LW jams (H2c). If dense forest stands limit transport of LW pieces onto the floodplain, jam size may be smaller and more commonly composed of CPOM as opposed to LW.

2. Study Area and Methods

2.1. Study Area

Our sites are located in the montane region (1,750–2,850 m) of the West Creek drainage basin in the CFR (Figure 2). The CFR is characterized by a semiarid climate, with temperatures averaging between −10–0 °C in winter and 10–22.5 °C in summer, depending on elevation (Sibold et al., 2006; Veblen & Donnegan, 2005). Annual precipitation ranges from 116 to 825 mm with an average of 389 mm (Colorado Climate Center of Colorado State University, 2019). Peak stream flows are primarily snowmelt driven and occur in the spring months. Scattered but intense summer thunderstorms can temporarily increase stream flows (Sibold et al., 2006). In the montane zone, dominant tree species include ponderosa pine (*Pinus ponderosa*) and Douglas-fir (*Pseudotsuga menziesii*) (Buechling & Baker, 2004; Veblen & Donnegan, 2005). Basin lithology is characterized by Silver Plume Granite deposited during Mid-Proterozoic volcanism (Boos & Boos, 1934; Braddock & Cole, 1990). Glacial till and moraines are present at higher elevations (Braddock & Cole, 1990; Jones & Quam, 1944).

West Creek has a drainage area of 59 km^2 and flows into the North Fork of the Big Thompson River, with the drainages contributing to the Big Thompson and then South Platte Rivers. West Creek is ungaged and flows through a well-defined valley. The upper portion of the catchment is located within the Rocky Mountain National Park, and the lower portion of the river is located within the Roosevelt National Forest. As the Cow Creek tributary (drainage area = 25.3 km^2) flows into West Creek, the drainage area increases by ~80% (Figure 1). Historical fires dating back to the 1,300 s have been recorded in the basin (Buechling & Baker, 2004), but most recently, the Cow Creek Fire burned 1,200 acres upstream of our study area in

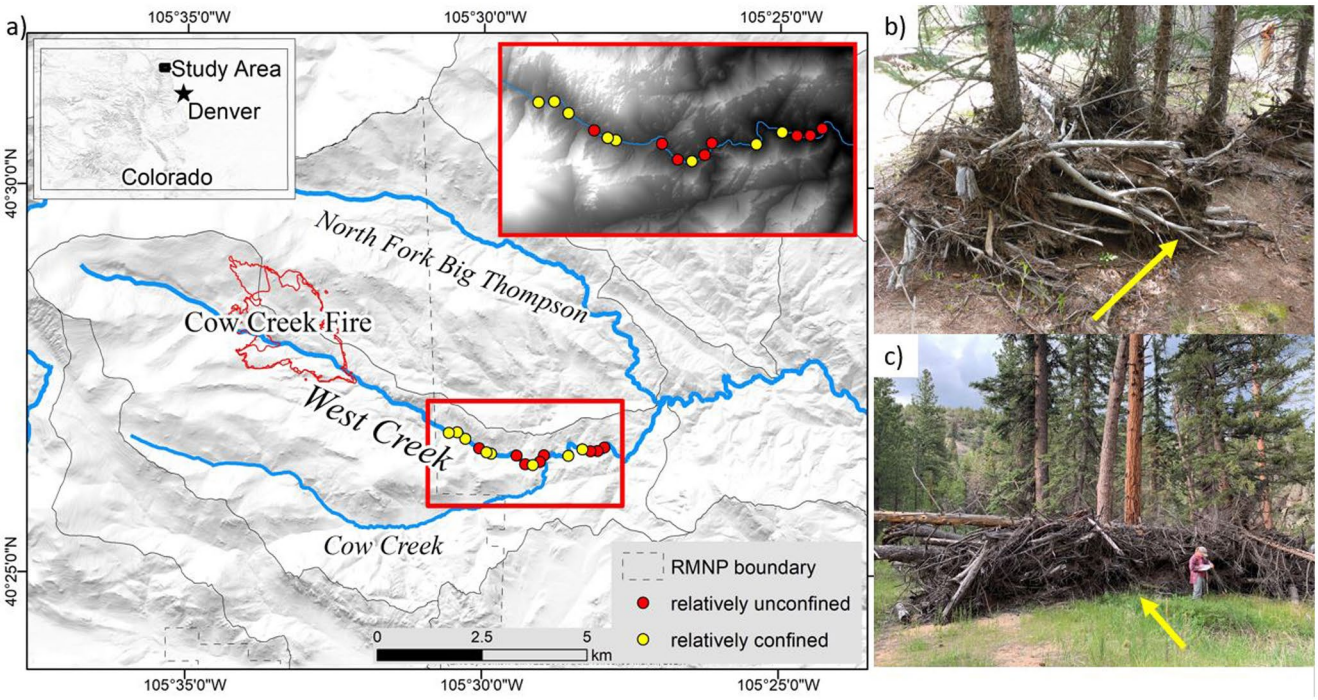

Figure 2. Study area, showing West Creek flowing into the North Fork Big Thompson River and the location of the study reaches (a), and photos of jams comprised mainly of CPOM (b) or LW (c). Yellow arrows in photos show streamflow direction at each location. The CPOM jam is ~0.5-m high and does not contain 3 or more pieces of LW (>1 m in length and >0.1 m in diameter), and the LW jam is ~2-m high, showing a person for scale. LW, large wood; CPOM, coarse particulate organic matter.

2010. In September 2013, an unusual amount of rain (up to 457 mm) fell over the CFR over multiple days, culminating in a 400-years flood event on West Creek (Yochum & Collins, 2015; Yochum & Moore, 2013). Peak flood discharge was estimated as 311.49 $m^3 s^{-1}$ near the outlet of West Creek, using the critical depth equation and cross sections of the flooded surface based on high water marks, such as bent grass and slack water deposits (Yochum & Moore, 2013). A 400-years recurrence interval was estimated using a regional regression equation for peak flow prediction (Capesius & Stephens, 2009; Yochum & Moore, 2013). This flood deposited large amounts of floodplain LW and CPOM jams on West Creek, providing an opportunity to characterize floodplain jams in relation to geomorphic and forest stand characteristics. We limited our fieldwork to the lower portion of the West Creek drainage; upstream of our study area, there is a knickpoint and the valley becomes very confined and steep, impeding our access to upstream reaches. We noted that there were LW and CPOM jams deposited from the knickpoint to the outlet of West Creek along with channel erosion, some local hillslope failures, and sediment deposition from the flood. This indicates that the 2013 flood clearly had enough energy to entrain, transport, and deposit wood throughout the study region. We suspect that at least some LW was sourced relatively near the sites of deposition due to observations of floodplain and hillslope erosion from the flood, and we noted LW pieces with connected roots.

2.2. Fieldwork

Prior to data collection in the field in Summer 2019, we used remote data sets to determine measurement locations. The West Creek valley bottom was delineated using NAIP aerial imagery and a high-resolution digital elevation model (1 m) created from lidar flown after the 2013 flood. We placed points every 100 m along the river channel line using GIS software along a 6.2-km length of stream downstream of the knickpoint, resulting in 62 potential points for locating study reaches. We classified each point as being located within a relatively confined or relatively unconfined valley bottom based on the valley bottom delineation, and these preliminary classifications were used to create confined (22 points) and unconfined (43 points) strata from which points were randomly selected for field measurement. In the field, we used these selected points as locations within which ~100-m long reaches were established. We ensured that each reach

represented relatively consistent confinement within the 100 m reach length; a few reaches were <100 m in length due to this criterion. We used the preliminary GIS analysis and relative confinement classification to ensure that we randomly selected locations representative of the variability in valley bottom confinement, but we determined the extent of the study reaches in the field and measured confinement in the field (not with the initial confinement categorization). Thus, the initial confinement categorization was not used when analyzing the data. We have included the distance between each study reach in Table S1.

We completed measurements on eight relatively unconfined reaches and eight relatively confined reaches (based on our GIS analyses described above), measuring geomorphic characteristics of each reach (reach-level data) and LW and CPOM loads in all jams within the reaches ($n = 193$ jams). We did not see evidence of reworking or burial of floodplain jams since the flood in 2013. Reach-level measurements included average bankfull width and average valley bottom width on river left, measured with either a laser rangefinder (TruPulse 360B) or a metric tape along five equally spaced transects perpendicular to the channel. We identified the current bankfull channel by assessing breaks in slope and vegetation characteristics. Due to high water conditions, we limited our measurements to river left (RL) and did not include measurements on the opposite side of the valley (river right). Thus, our average valley bottom width only incorporates the valley bottom width on RL. We are confident that limiting ourselves to one side of the valley did not bias our results because our approach to randomizing site selection within strata captured the range of variability in confinement along RL. We observed that the RL valley bottom did not systematically differ from the valley bottom on river right in a way that would bias our results. We used the ratio of the average RL valley bottom width to the average bankfull width as an RL confinement index in further analyses. We also measured the basal area of live trees in the floodplain forest with a Panama angle gage to calculate forest stand density ($m^2\ ha^{-1}$) along the five equally spaced transects perpendicular to the channel, stopping the measurements at the edge of the valley bottom. There were very few standing dead trees in the floodplain. Average slope of the channel for each reach ($m\ m^{-1}$) was also measured using the laser rangefinder. We determined the drainage areas for each of the reaches using the US Geological Survey's StreamStats web application.

We also measured jam-level characteristics for all jams within the study reaches (jam-level data). A set of rules and definitions were established in the field to simplify jam identification and measurement. First, two types of jams were defined: CPOM jams and LW jams (Figures 2b and 2c). A LW jam contains three or more connecting pieces of LW. Many LW jams also contained some CPOM, but the significant proportion of LW in the jams warranted their classification as LW jams. Thus, LW jams contain some CPOM, but we did not differentiate between CPOM and LW within the LW jams. Conversely, a CPOM jam is primarily composed of material smaller than LW and <3 LW pieces are present within the jam. Within each study reach, we measured all LW and CPOM jams larger than a minimum size. Jams were only measured if at least 2 of the 3 dimensions (length, width, or height) were greater than 0.5 m, thereby excluding very small jams.

To measure each jam's volume, three dimensions were defined relative to the stream. Jam length is the dimension most parallel to streamflow, jam width is the dimension most perpendicular to streamflow, and jam height is simply the average distance from the ground to the top of jam. These three dimensions approximated a best-fit box around the jam (Livers et al., 2020). LW and CPOM volume in each jam was calculated by multiplying best-fit box volume by the proportion of filled space (1-porosity) (Livers et al., 2020). Two researchers independently estimated porosity visually in intervals of 5%, and we averaged the two measurements to determine LW and CPOM jam volumes. We used a percentage diagram for estimating composition by volume (Compton, 1985) at the beginning of our fieldwork to help with our porosity estimates. Individual pieces of wood that extended beyond the main portion of the jam (tails) were not included in the dimension measurements of the jams. Tails were instead "cut off" at the last intersection with another piece of LW in the jam. If a tail extended to touch a nearby jam, the tail was noted but the jams were recorded separately. If multiple (≥2) tails connected two jams, the jams were recorded as multiple parts of the same jam. However, if parts of a multipart jam were classified differently as LW or CPOM, those multipart jams were recorded as separate jams in order to distinguish between primarily LW or CPOM jams. We also measured the local bankfull channel width associated with each jam, measuring width at the closest channel location to the jam.

We also assessed whether the jams were pinned against a stable feature, and if so, what the pinning mechanism was (e.g., standing tree, valley wall, bedrock outcrop, etc.). For jams pinned by trees, we measured

the diameter at breast height (DBH; cm) of the trees. If multiple trees pinned a jam, we summed the DBH of the pinning trees to determine the total blockage (in cm) for the jam. For each jam, we also measured the distance between the jam center and the bankfull channel edge (distance from channel) and the elevation of the jam base above the bankfull channel edge (elevation above channel) using the laser rangefinder. We noted whether any LW pieces in the jams had rootwads attached to them, whether the jams had any vegetation growing on them and the type of vegetation (herbaceous or wood), and the dominant decay class of any LW pieces within the jam. Decay class categorization followed the classes described in the WooDDAM database framework (Scott et al., 2019), which is based on Harmon et al. (2011). Decay classes range from 1, which is very little decay, to 5, which describes rotten wood with a soft texture. See supporting information Text S1 for a full description of decay classes. Finally, we noted whether any LW pieces were charred to determine whether the LW was sourced from the Cow Creek fire area upstream of our study locations; we only noted a few LW pieces with charring. Although we cannot definitively conclude that an absence of charred wood in our study region indicates a lack of wood transport from the upstream fire area to our study reaches, it is probably that most of the LW in jams was sourced from areas downstream of the fire location.

2.3. Statistical Analyses

We employed nonparametric statistical tests to evaluate correlations between jam-level and reach-level variables to account for the nonnormal distribution of most measured variables. At the jam scale, we used Spearman correlation tests to determine the significance and magnitude of a monotonic relationship between jam volume (m^3) and the following variables: elevation of the jam above the bankfull channel (m), distance from the jam to the channel (m), bankfull channel width at the closest channel location to the jam (m), and the total blockage (sum of the DBHs) of the jam due to trees (cm). A Kruskal-Wallis *H* test was used to determine whether there was a significant increase in jam volume with increasing number of tree pins.

At the reach scale, we calculated the following response variables: total jam load (m^3), jam load per area (m^3 ha^{-1}), jam count (number), and jam count per area (number per ha). Spearman correlation tests were then used to investigate the magnitude and significance of the relationships between the four response variables and the following reach-level variables: river left (RL) confinement index (the ratio of average valley bottom width on river left to average bankfull channel width, meaning that lower values indicate more confined channels; m m^{-1}); average slope (m m^{-1}); drainage area (km^2), which is a proxy for the upstream source of water and wood inputs; and basal area (m^2 ha^{-1}). We also tested whether there was a nonlinear relationship between the four response variables and basal area using a polynomial regression. Tests were performed separately by jam type (LW and CPOM). To determine if there were significantly more LW jams (jam count) or a significantly larger LW jam load (total jam load) compared to CPOM jams, we used a Wilcoxon test.

The relative influence of river corridor geomorphology versus forest stand characteristics on jams at the reach scale was tested using all subsets model selection on multiple linear regressions. Regression models were created for jam count, jam count per area, total jam load, and jam load per area using data sets for both jam types (LW and CPOM) combined. To control for patterns driven by CPOM versus LW jams, we included the proportion of CPOM jams as a predictor variable. All morphology and forest covariates that were noncollinear were included as predictor variables in the full models. We used the variance inflation factor (VIF) as an indicator for collinearity, removing one variable from the model at a time and reassessing the VIF if any variables had a VIF of ~4 or above. Cutoffs for VIF values range from 3 to 10, but higher VIF values are a good indicator of collinearity of predictor variables (Thompson et al., 2017).

Total jam load and load per area full models included drainage area, jam counts, average channel slope, RL confinement index, basal area, and proportion of CPOM jams in each reach as potential predictor variables. Average bankfull width was removed due to collinearity. Because both jam types were included in the response variables of the models, the proportion of CPOM jams was included as a predictor to account for variations in jam type in each reach. To meet model assumptions, total jam count and jam count per area response variables were square root transformed. Total jam count and jam count per area full models included drainage area, average jam size, RL confinement index, basal area, and proportion of CPOM jams. Average bankfull width was removed due to collinearity from these models as well. All subsets model selection was

performed on each model using the *dredge* function in the MuMIn R package, which automates model selection and ranks the models with information criteria (Barton, 2019).

We considered all models with an Akaike information criterion corrected for small sample sizes (AICc; Hurvich & Tsai, 1989) within 2 units of the lowest criterion value. We selected the best model as the one within this range that contained the fewest predictor variables. We ranked the importance of model predictor variables by summing the Akaike weights (Wagenmakers & Farrell, 2004). All tests and models were evaluated at a significance level of 0.05 ($\alpha = 0.05$). We also report and note p-values that are less than $\alpha = 0.10$ to assess additional, albeit weaker, patterns, and trends in the data, in part due to recent criticism of arbitrarily selecting significance levels (e.g., Krueger & Heck, 2019). We also rely on interpretation of graphical relationships in addition to statistical tests in order to interpret our results.

3. Results

3.1. General Characteristics of Jams and Reach-Level Data

Average LW and CPOM volumes of individual jams were 9.78 m^3 (standard error (SE) = 2.6; median = 0.93 m^3) and 0.43 m^3 (SE = 0.09; median = 0.23 m^3), respectively. At the reach scale, LW loads per area ranged from 0 to 2,624 m^3 ha^{-1} (mean ± SE = 678.6 ± 192.3 m^3 ha^{-1}; median = 382.1 m^3 ha^{-1}), and CPOM loads per area ranged from 0 to 80 m^3 ha^{-1} (mean ± SE = 10.7 ± 4.8 m^3 ha^{-1}; median = 5.0 m^3 ha^{-1}), with a higher average load per area for LW jams compared to CPOM jams ($p < 0.001$). Overall, LW jam count per area was higher than CPOM jam count per area for all reaches ($p < 0.001$), with an average of 70.4 ± 0.2 LW jams ha^{-1} and 19.0 ± 3.7 CPOM jams ha^{-1}. Most LW in jams had a decay class of 2 (76.8% of jams) or 3 (16.0% of jams), indicating that the heartwood can still support its own weight despite some wood decay. This implies that the wood was likely deposited in the 2013 flood. Many jams had plants growing out of the jam (55.7%), and almost all observed plants were herbaceous, with only one or two jams having woody seedlings. We identified a rootwad within 47 out of 193 jams (24.3%). The two independent estimates of jam porosity completed by different field researchers were very similar, with average porosity of all jams being 0.51 for both observers (Figure S1). However, at low porosities (<20%) and high porosities (>75%), the two estimates differ more substantially. Geomorphic and forest stand characteristics of the study reaches are shown in Table 1, with summary statistics for CPOM and LW reach-level and jam-level data in Tables S2 and S3, respectively. Correlations between reach-level and jam-level are included in Data Set S1 and S2 in supporting information. Although there is a large jump in drainage area downstream of the confluence with Cow Creek, the average bankfull width, slope, and RL confinement index did not vary systematically with drainage area (Figure S2), likely due to the limited range of drainage areas of the study reaches.

3.2. Influence of River Corridor Geomorphology on Floodplain Jams

For individual jams, LW jam volumes have a significant inverse correlation with elevation above and distance from the channel ($p < 0.001$ and $\rho = -0.3$ and -0.35, respectively) (Figures 3a and 3b). Thus, the size of LW jams decreased as distance from the channel and elevation above the channel increased. However, there was not a similar significant trend in CPOM jam size with elevation above and distance from the channel ($p = 0.49$ and $p = 0.71$, respectively) (Figures 3a and 3b). LW jam volumes have a significant direct correlation with bankfull width ($p < 0.001$ and $\rho = 0.27$); essentially, larger LW jams formed where the proximal bankfull width was wider (Figure 3c). A similar relationship between jam volume and bankfull width did not exist for CPOM jams ($p = 0.23$ and $\rho = 0.18$, Figure 3c).

At the reach level, reaches with less lateral confinement (higher value of ratio of average valley bottom width to average bankfull width) had higher jam counts of both LW ($p = 0.004$; $\rho = 0.67$) and CPOM jams ($p = 0.001$; $\rho = 0.73$) and higher total jam loads of both LW ($p = 0.01$; $\rho = 0.61$) and CPOM ($p = 0.06$; $\rho = 0.47$) (Figure 4). However, when normalized by floodplain area, there was no trend in jam counts per area or loads per area for either jam type with RL confinement index (Figure 4). Additional significant correlations included an increase in the total jam load (LW: $p = 0.02$, $\rho = -0.59$; CPOM: $p < 0.001$, $\rho = -0.75$) and an increase in jam count (LW: $p = 0.03$, $\rho = -0.52$; CPOM: $p < 0.001$, $\rho = -0.75$) with decreasing slope (Figure 5). A similar but weaker relationship existed between jam load normalized for area and slope (LW: $p = 0.09$, $\rho = -0.43$; CPOM: $p = 0.08$, $\rho = -0.44$). Jam count per area was lower in reaches downstream

Table 1
Geomorphic and Forest Stand Characteristics of the Study Reaches

Reach number	Reach length (m)	Drainage area (km^2)	Average bankfull width (m)	Slope ($m\ m^{-1}$)	RL confinement index	Basal area ($m^2\ ha^{-1}$)
28	100	58.0	9.1	0.030	2.98	11.82
30	100	57.8	10.4	0.033	1.61	10.33
32	70	57.7	9.0	0.046	0.84	0.00
34	90	57.6	7.8	0.023	1.56	7.10
42	100	57.0	7.3	0.051	0.51	0.26
49	100	56.7	6.9	0.021	4.71	17.49
50	100	31.3	29.9	0.025	0.90	23.56
52	75	30.0	4.7	0.055	0.33	6.89
54	100	29.8	4.9	0.027	4.47	16.07
57	100	29.0	8.4	0.036	1.42	10.33
65	100	28.7	5.9	0.039	0.78	8.90
66	68	28.5	7.0	0.043	0.38	6.89
69	100	31.1	8.1	0.035	1.52	7.24
73	100	31.0	7.7	0.027	3.51	17.18
76	100	30.8	7.6	0.023	0.67	8.93
78	100	30.0	10.0	0.036	1.13	15.86

of the confluence with Cow Creek, with drainage areas greater than 56 km^2, ($p = 0.005$; $\rho = -0.66$), but there were no other significant relationships between reach-level jam response variables and drainage area (Figure S3). There is a large jump in drainage area across our sites, due to the entrance of the Cow Creek tributary along West Creek. The reach-level jam response variables (total jam load, jam load per area, jam count, and jam count per area) did not have any significant correlations with average bankfull width.

3.3. Influence of Forest Stand Characteristics on Floodplain Jams

A majority of floodplain jams (64% of LW jams and 72% of CPOM jams) were pinned by at least one object. Most pinned LW jams and all pinned CPOM jams were pinned against trees, but a small percentage (2.7%) of LW jams were pinned on other objects such as boulders and sandbars. The highest number of pins recorded was 14 trees, which occurred at one measured LW jam. Although there was a significant correlation between jam volume and number of tree pins ($p < 0.001$ and $p = 0.04$ for LW and CPOM, respectively), there was no significant difference in volume between unpinned jams and jams pinned only once by trees ($p = 0.9$ for both jams types). This indicates that multiple trees are needed to provide a pinning mechanism to significantly increase jam volumes (Figure S4). As total blockage, which is the sum of the DBHs of the pinning trees, increases, jam volume increases for LW jams ($p < 0.001$; $\rho = 0.50$) but not for CPOM jams ($p = 0.16$, $\rho = 0.21$) (Figure S4).

We did not find a significant nonlinear trend between basal area and total jam load, jam load per area, jam count, or jam count per area for either jam type (Figure 6). We had expected a nonlinear trend because we expected that an intermediate floodplain forest stand density promotes the highest floodplain jam loads and counts, since trees serve as trapping locations but dense stands would impede transport into the floodplain. Spearman correlations were used to further investigate a monotonic relationship, which would mean that there is an increasing or decreasing trend that may not necessarily be linear. LW and CPOM jam counts significantly increase with increasing basal area (both $p < 0.001$, Figure 6). CPOM jam count per area was also found to increase with basal area ($p = 0.06$), but LW jam count per area did not ($p = 0.42$). Additionally, the average size of CPOM jams significantly increases with increasing basal area ($p = 0.01$), while basal area did not have a significant effect on LW jam size ($p = 0.29$) (Figure 6e). The proportion of total jams comprised of CPOM jams increases with basal area ($p = 0.03$) (Figure 6f).

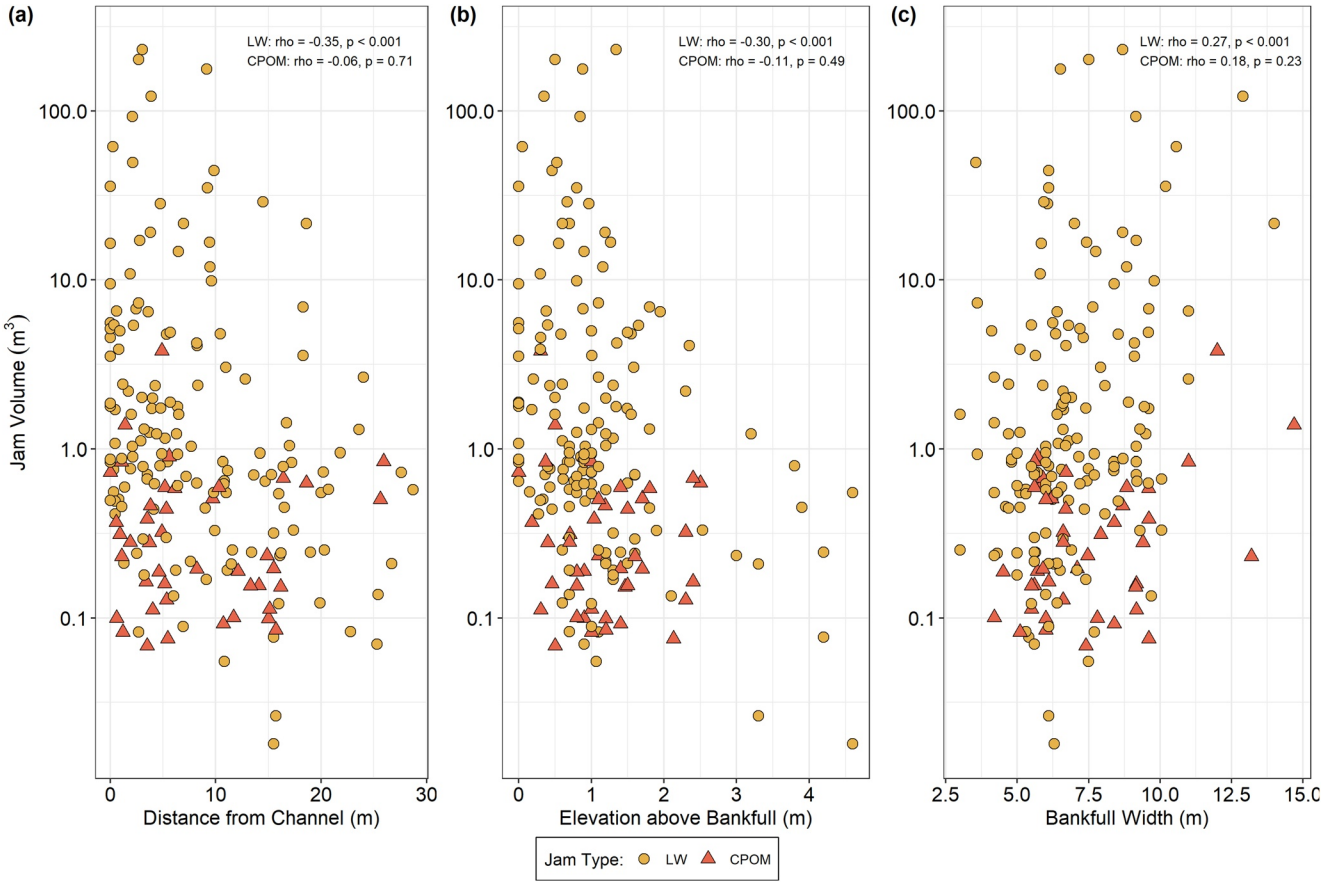

Figure 3. Plots of jam volume (log-transformed) versus distance from channel (a), elevation above bankfull channel (b), and bankfull width at the channel location closest to the jam (c) based on individual jam data.

3.4. Comparing the Influence of River Corridor Geomorphology and Forest Characteristics on Floodplain Jams

To assess the relative influence of river corridor geomorphology and forest characteristics on floodplain jams, we used multiple linear regression models with the four reach-level jam variables as response variables (total jam load, load per area, jam count, and jam count per area). We used multiple linear regression models to identify the association between the response variables and individual predictor variables while accounting for the interplay between predictor variables, as well as to access the relative importance of each predictor variable. Final models for total load and load per area included reach averaged channel slope as the only significant predictor variable (Table 2). Total jam load and load per area decrease with increasing channel slope (Figure 5). When summing the Akaike weights for all predictor variables for the total jam load all subsets models, the relative ranked importance of the variables for the total load model were slope (sum = 0.86), proportion CPOM jams (sum = 0.25), RL confinement index (sum = 0.19), basal area (sum = 0.15), and drainage area (sum = 0.12). The relative ranked importance for all predictor variables for the load per area model were slope (sum = 0.71), basal area (sum = 0.29), drainage area (sum = 0.25), proportion CPOM jams (sum = 0.17), and RL confinement index (sum = 0.16). The final jam count model chosen through AICc included only basal area as a predictor variable; this model had the best fit of all four models ($R^2 = 0.71$). As basal area increases, jam count increases (Figure 6). Using the sum of the Akaike weights for the all subsets models, the ranked importance for the jam count model were basal area (sum = 1.00), proportion CPOM jams (sum = 0.55), average jam size (sum = 0.12), drainage area (sum = 0.11), and RL confinement index (sum = 0.11). The jam count per area final model chosen with AICc includes drainage area as the only predictor, and the ranked importance of variables using Akaike weights were drainage area (sum = 0.96), basal area (sum = 0.18), RL confinement index (sum = 0.13), average jam size (sum = 0.13),

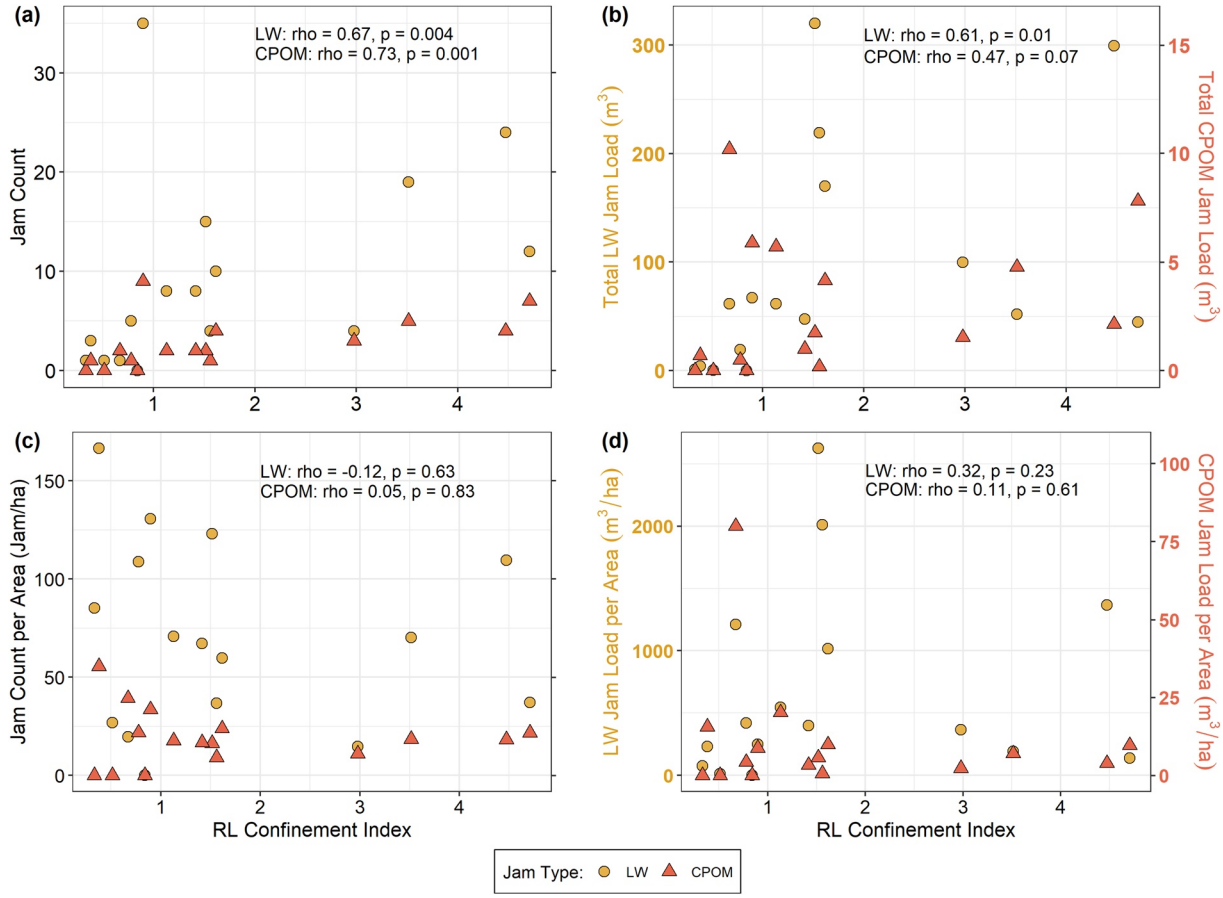

Figure 4. Plots of jam count (a), total jam load (b), jam count per area (c), and jam load per area (d) versus RL confinement index using reach-level data. RL confinement index is the ratio of the valley bottom width on river left to channel width. Note that plots (b) and (d) have two *y* axes to better show trends in both the LW and CPOM loads. RL, river left; LW, large wood; CPOM, coarse particulate organic matter.

and proportion CPOM jams (sum = 0.13). Jam count per area significantly decreases with increasing drainage area at West Creek.

4. Discussion

Our results indicate that both river corridor geomorphology and floodplain forest stand characteristics influence individual jam characteristics and the load and number of floodplain jams, providing support for some of the hypotheses described in Section 1.

4.1. Geomorphic and Forest Stand Controls on Individual Jam Characteristics

Individual LW jam size decreased with increasing distance from and elevation above the channel, but a similar trend was not found for CPOM jams (Figure 3). Smaller CPOM was carried and deposited a range of distances during the 2013 flood, while more LW pieces were deposited closer to the channel. Studies on wood mobility and transport have found that the relationship between wood piece dimensions and flow characteristics can influence transport (Braudrick & Grant, 2001). For example, the ratio of flow depth to wood piece diameter is an important influence on wood mobility (Dixon & Sear, 2014; Iroumé et al., 2018; Wohl & Goode, 2008). Thus, as flow depth and velocity decreased from the channel onto the floodplain during the flood, LW deposition likely occurred and fewer LW pieces were transported into the distal floodplain. Because CPOM is smaller and more easily transported by slower flows, CPOM jams were deposited in a range of distances from the channel. The pattern of LW deposited near the channel with CPOM deposited

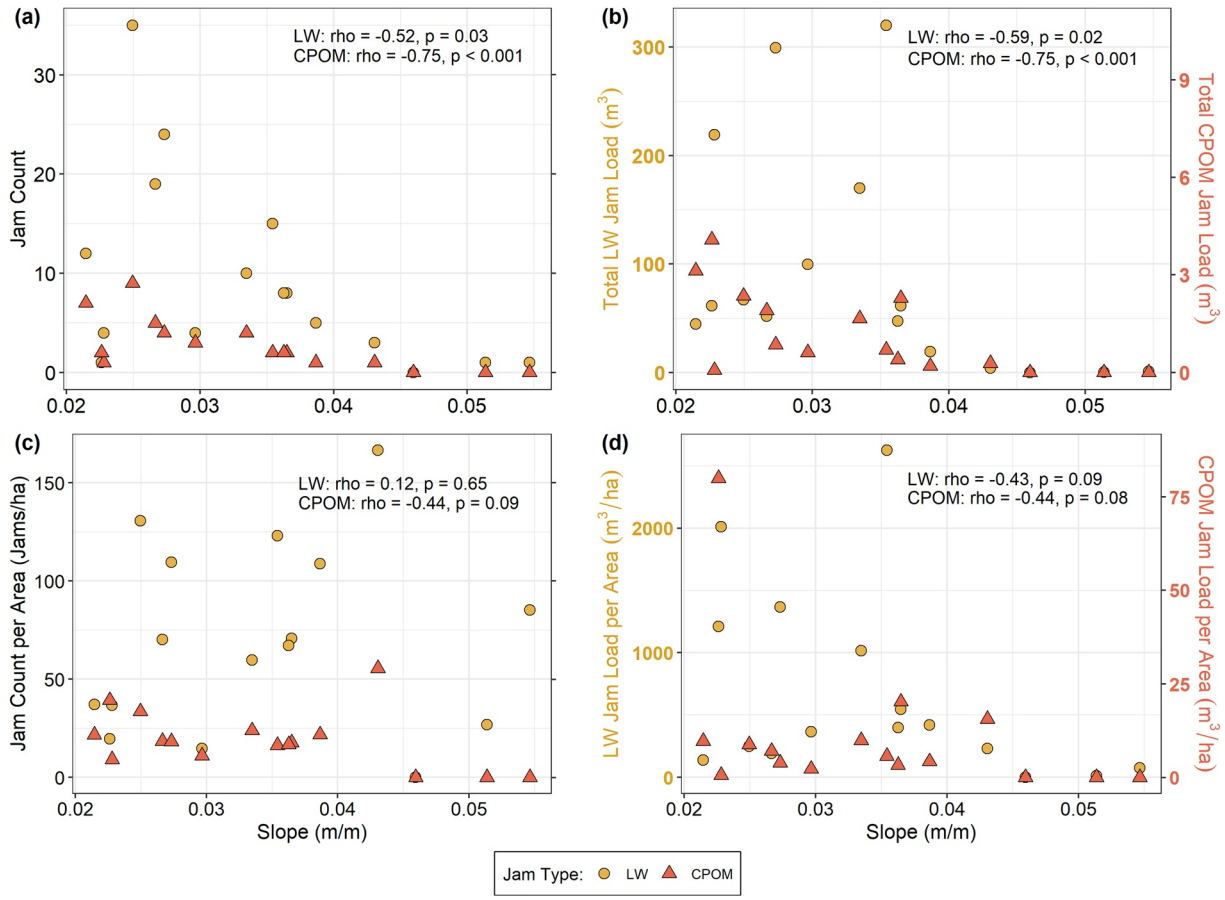

Figure 5. Plots of jam count (a), total jam load (b), jam count per area (c), and jam load per area (d) versus slope using reach-level data. Note that plots (b) and (d) have two *y* axes to better show trends in both the LW and CPOM loads. LW, large wood; CPOM, coarse particulate organic matter.

both near and far from the channel is somewhat similar to the commonly observed trend in grain sizes from the channel margin to the distal floodplain, with coarser particles deposited closer to the channel (e.g., sands) and finer particles transported further from the channel (e.g., silts and clays) (Gurnell, 2007; He & Walling, 1998; Pizzuto, 1987). Larger individual LW jams formed where the bankfull width closest to the jam was wider, but this relationship was not present with CPOM jams (Figure 3c). This relationship may indicate that wider channel locations resulted in decreased flow velocities and flow depths, promoting LW deposition nearby on the floodplain, although further exploration is needed.

The majority of floodplain jams, both LW and CPOM, were pinned by trees. This indicates the important role that valley bottom trees can play in storing LW and CPOM. In addition, when multiple trees pinned a jam, that jam tended to be larger (Figure S4). Vegetation served as pinning mechanisms for large LW volumes in the Sabie River in South Africa and in sites in New Mexico, USA as well (Pettit et al., 2005; Wohl et al., 2018a), supporting our findings. Approximately one-fourth of the jams (24.3%) had rootwads in them, pointing to the high numbers of trees that were likely uprooted during the flood from the valley bottom and then redeposited.

One interesting observation is that floodplain LW jams measured on West Creek can be four to five times larger than in-channel wood jams in the CFR. In-channel LW jam volumes in CFR streams with similar drainage areas (10–175 km^2) to West Creek ranged from 0.02 to 49.8 m^3 (Livers et al., 2020), and the floodplain LW jams measured here range in volume from 0.02 to 231.75 m^3. Initial observations in the CFR indicate that there are not comparably large in-channel jams created by the flood, since the flood likely caused in-channel wood transport and may have broken up larger in-channel jams. However, more work is needed to compare in-channel and floodplain jam characteristics.

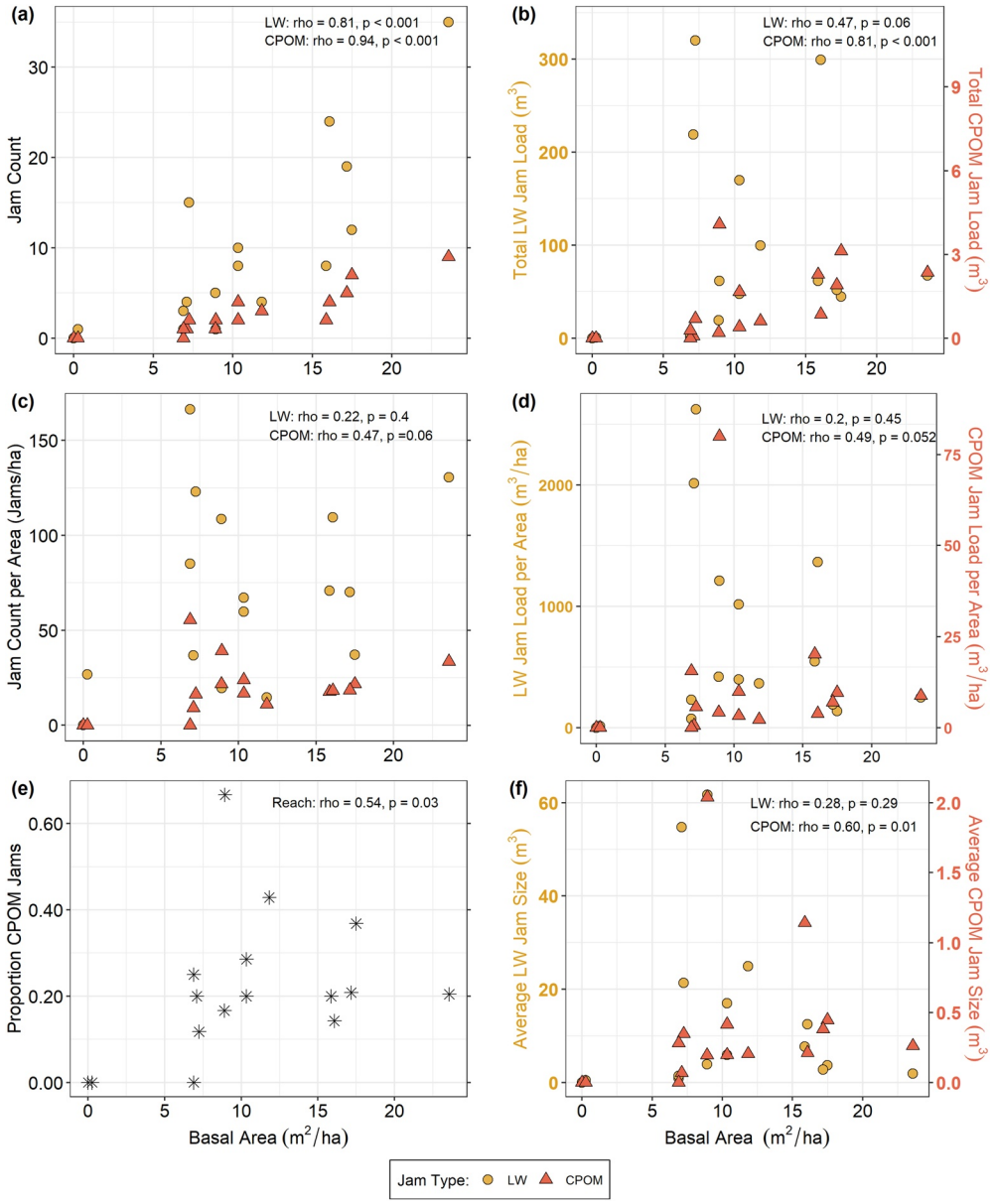

Figure 6. Plots of jam count (a), total jam load (b), jam count per area (c), jam load per area (d), average jam size (e), and the proportion of CPOM jams (f) versus basal area, using reach-level data. Note that plots (b), (d), and (f) have two *y* axes to better show trends in both the LW and CPOM loads. LW, large wood; CPOM, coarse particulate organic matter.

Table 2
Model Summaries of the Four Reach-Level Jam Response Variables

Response variable	Variables included in final model (*p*-value) [coefficient β]	Multiple R^2 for final model	Top variables ranked with importance
Total load[a]	Average slope (0.007) [−351.98]	0.41	Slope, proportion CPOM jams
Load per area[a]	Average slope (0.041) [−723.48]	0.27	Slope, basal area, drainage area
Jam count	Basal area (<0.0001) [1.79]	0.71	Basal area, proportion CPOM jams
Jam count per area	Drainage area (0.002) [−2.91]	0.49	Drainage area, basal area

[a]Total load and load per area models were square root transformed to satisfy model assumptions.

4.2. Geomorphic and Forest Stand Controls on Reach-Scale Jam Loads and Counts

We initially hypothesized that unconfined reaches would have higher jam loads and counts. In the Sabie River in South Africa, wider "macro-channels," which are defined as the valley bottom width that includes the perennial channel and smaller ephemeral channels, contained more LW volume deposited after a flood compared to more confined reaches (Pettit et al., 2005). Our results suggest that slope plays a more important role in influencing jam loads compared to confinement. However, the range in RL confinement is relatively small on West Creek, thus slope may play a more important role within this narrower range of confinement values. As slope increased, total load, load per area, and jam count decreased (Figure 5 and Table 2). Slope and confinement tend to be related and are correlated in our study reaches ($\rho = -0.66$, $p < 0.05$; Data Set S1), with higher slopes in more confined reaches, but our univariate comparisons and model analyses indicate that slope may be a more important control. Slope is also inversely correlated with basal area ($\rho = -0.69$, $p < 0.05$; Data Set S1).

Previous work has related the unit stream power (the product of discharge, slope, and the specific weight of water, divided by channel width) to patterns of deposition and erosion of sediment during flood events, with higher unit stream power resulting in greater erosion and fluvial change (Cenderelli & Wohl, 2003; Sholtes et al., 2018). Thus, decreased slope indicates a decrease in the unit stream power that a reach experiences during a flooding event, potentially allowing for greater deposition of LW and CPOM. Unit stream power gradient, or the change in unit stream power from reach to reach, also influences fluvial change in river corridors (Sholtes et al., 2018). However, LW has greater buoyancy than sediment transported on the riverbed and can float in water (Ruiz-Villanueva et al., 2016), complicating the explanation that stream power influences LW deposition during flooding in the same manner as sediment. Nevertheless, the correlation between LW and CPOM loads and slope point to potential mechanisms such as lower stream power or decreasing stream power resulting in LW and CPOM deposition. For example, a downstream decrease in stream power could have resulted in decreased transport capacity or created lateral eddies that deposited LW and CPOM. In contrast to our finding that decreased slope resulted in higher LW and CPOM loads, valley bottom LW volumes on the Sabie River were higher in bedrock anastomosing reaches that had higher reach slopes, but this is likely due to the greater presence of trapping mechanisms such as bedrock outcrops and vegetation in these reaches (Pettit et al., 2005). On West Creek, reaches with steeper slopes had lower basal area, indicating that steeper reaches have fewer trapping locations for jams.

Drainage area was significantly associated with LW jam count per area, and was the only variable chosen in the final model of jam count per area (Figure S3 and Table 2). As drainage area increased, LW jam count per area decreased. Drainage area did not have a significant correlation with load per area or average jam size (Data Set S1), and average bankfull width, slope, and RL confinement index did not scale with drainage area (Figure S2). The relationship between drainage area and jam count per area is difficult to explain, because we would expect that as jam count per area decreased, load per area or average jam size would also change. For example, as jam count per area decreases downstream, we would expect that either load per area would decrease or average jam size would increase. The lack of change in load per area indicates that LW inputs to each reach did not significantly change from upstream to downstream. Although we did not assess LW sourced during the flood, field observations indicate that LW likely was recruited from eroded valley bottoms and hillslope failures. There is a large increase in drainage area across our reaches due to a tributary (Cow Creek) joining West Creek, but it may be that we do not have a wide enough range in drainage area values to discern relationships between drainage area, LW load, and LW jam size, and LW counts.

Our results suggest that CPOM deposition and jam formation occur in locations with denser valley bottom forests, but the relationship is more complicated for LW jams. CPOM jam count and load normalized by area (but not LW count and load normalized by area), the proportion of CPOM jams, and the average size of CPOM jams increased with increasing basal area, demonstrating that trees are important pinning locations for CPOM jams (Figure 6). The final model for jam count included basal area as a predictor variable, and basal area had a high relative importance in the load per area full model. Although trees acting as pins influence LW jam formation, as described above, transport onto and through the floodplain can be impeded by standing trees. In addition, the spatial patterns and variation in tree locations on the valley bottom likely can influence LW jam deposition, but these influences probably play a smaller role in CPOM transport and deposition.

We hypothesized that an intermediate basal area would result in the highest jam loads and jam counts, but we did not find this relationship in our data. This could be due to a limited range of basal area measurements within our study reaches (range: 0–23.6 m^2 ha^{-1}; median = 9.6 m^2 ha^{-1}). Floodplains on streams with recent and older high-magnitude disturbances comparable to the West Creek disturbances (e.g., fire, floods) in New Mexico, USA had lower LW loads, particularly in jams, compared to West Creek, but also lower basal area values, with medians of 3.6 and 4.0 m^2 ha^{-1} (Wohl et al., 2018a). Floodplains with low-magnitude disturbances in Colorado, USA (e.g., snowmelt floods) had higher floodplain LW loads and higher basal areas (median of 8.5 m^2 ha^{-1}), but most of the floodplain LW was dispersed and was not concentrated into jams (Wohl et al., 2018a). In northern Montana, USA, floodplain LW jams were only common in abandoned channels, which the authors link to the high density of trees in the floodplain (Wohl et al., 2018b). These geographic comparisons indicate that high-magnitude disturbances may be required to form floodplain LW jams, but also that standing tree density likely plays a role in controlling the form and amount of LW on the floodplain. However, more work across diverse environments, coupled with physical and numerical modeling of LW transport onto floodplains, is needed to elucidate the competing controls of flood magnitude and basal area on floodplain LW. Our results highlight the need to better study how the location of individual trees and the density of trees influences floodplain jam formation and development, as well as the importance of preserving riparian forests to facilitate trapping of LW and CPOM accumulations.

We present a conceptual model that summarizes our main findings and that can be used as a framework for future research (Figure 7). LW and CPOM jam volume per area decreases in reaches with steeper slopes (Figure 7b), likely due to lower stream power during the flood, with lower forest stand density in reaches with steeper slopes. In reaches with less dense forests, there are fewer CPOM jams per area and a smaller CPOM jam volume per area due to a reduction in trapping locations for CPOM jams (Figure 7a). Finally, as distance from the channel and elevation above the channel increase, LW jam size decreases due to reduced transport capacity of floodplain flows, but there is no difference in CPOM jam size (Figure 7).

4.3. Comparing West Creek Jam Load to Other Floodplains

Although data on floodplain wood loads are limited for unmodified floodplains, and our study only measured floodplain LW load within jams, we can compare our results to other studies (Figure 8). These studies report values of LW load on floodplains, but only some investigate the geomorphic controls on LW loads. The average floodplain LW load in jams on West Creek is 678.6 m^3 ha^{-1}, which is much larger than many other published wood loads. For example, floodplains in the central Yukon River Basin contained on average 42 m^3 ha^{-1} of LW, but these data do not include floodplain-channel margin deposits (Lininger et al., 2017). Average floodplain LW loads in tropical and subtropical floodplains are somewhat lower, with values ranging from 28 to 50 m^3 ha^{-1} (Chao et al., 2008; Jaramillo et al., 2003; Wohl et al., 2011). However, large disturbances such as hurricanes can result in very high volumes of LW and CPOM within channels in subtropical and tropical environments, although we lack measurements of floodplain loads. For example, after Hurricanes Irma and Maria in September 2017, in-channel jams comprised of LW and CPOM resulted in loads of 40–2,224 m^3 ha^{-1} across 12 reaches in Puerto Rico (Wohl et al., 2019). Floodplains in humid temperate conifer forests in Montana, USA averaged 470–486 m^3 ha^{-1} of LW, most of which was dispersed across the floodplain and was not fluvially transported (Wohl et al., 2018b). Additional values of floodplain LW loads in the semiarid western USA range from 64 to 198 m^3 ha^{-1} (Lininger et al., 2017; Wohl, 2020; Wohl et al., 2018a). In one study, streams in the semiarid western USA with recent high-magnitude disturbance regimes that include fires and floods had average floodplain LW loads from 19 to 149 m^3 ha^{-1}, with average floodplain LW loads in low-magnitude disturbance regimes that include snowmelt floods ranging from 44 to 226 m^3 ha^{-1} (Wohl et al., 2018a). However, the high-magnitude disturbance sites had a higher proportion of LW in the floodplain as opposed to in the channel compared to the low-magnitude disturbance sites, as described above (Wohl et al., 2018a). The only location where measured floodplain LW loads were higher than the values reported here for West Creek is in northern California, USA, where very large redwood trees downed in the floodplain result in an average floodplain LW load of 743 m^3 ha^{-1} (Busing & Fujimori, 2005).

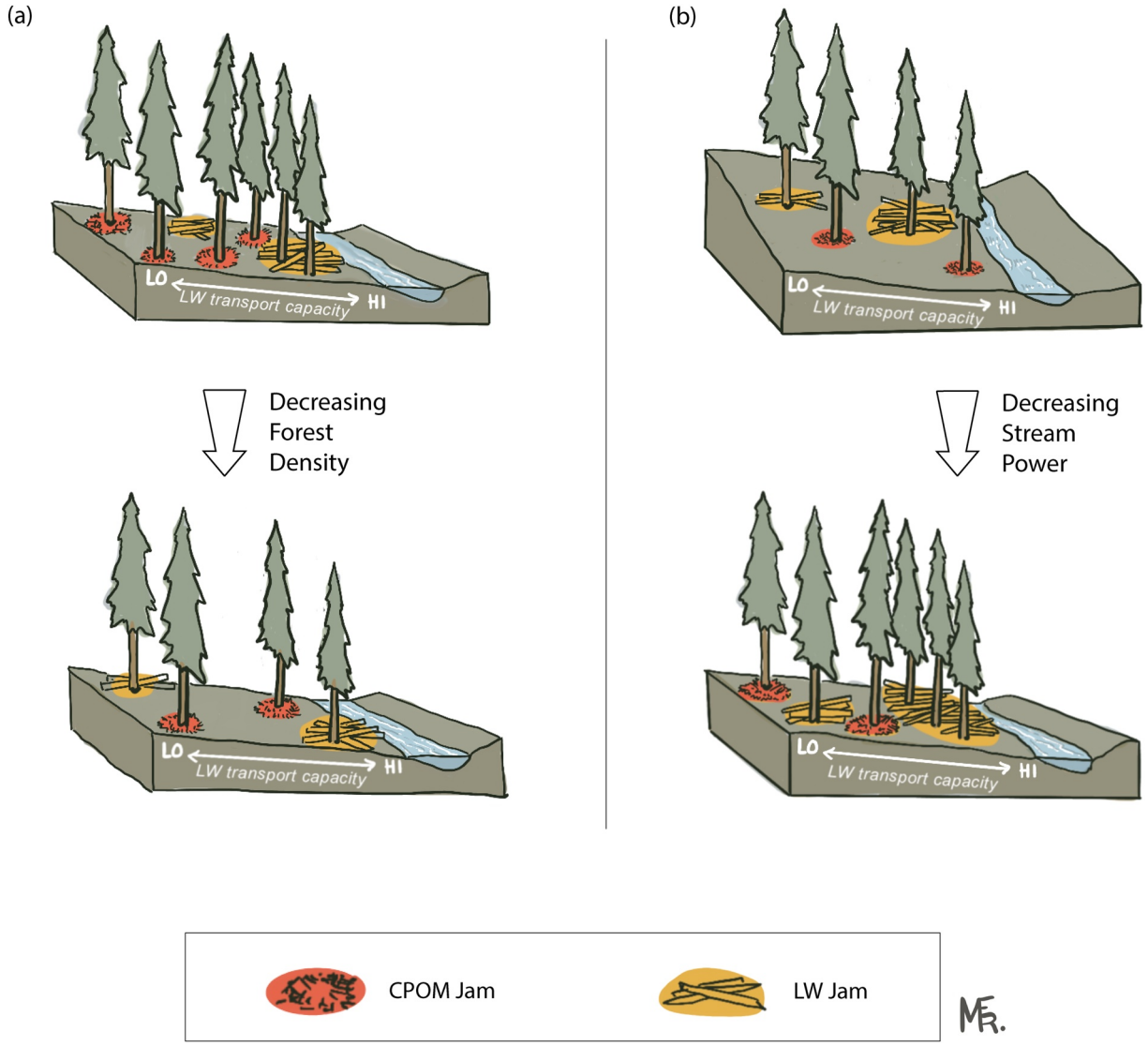

Figure 7. Conceptual model demonstrating the influence of forest density (a) and slope, which indicates reduced stream power during the flood (b) on floodplain large wood (LW) and CPOM (coarse particulate organic matter) jam depositional patterns. Illustration by Maisie Richards.

The very high LW load on West Creek compared to other locations emphasizes that high-magnitude disturbances such as fires and subsequent floods in semiarid river corridors can dramatically increase the amount of LW and CPOM stored on the floodplain. The upstream 2010 fire may have amplified the impact of the 2013 flood by enhancing runoff (Smith et al., 2011), increasing the transport and deposition of LW. One limitation of comparing West Creek to other environments is the lack of field studies measuring floodplain LW and CPOM following high-magnitude disturbance events and the difficulty in understanding the disturbance histories of previously studied locations. The deposited LW on West Creek showed relatively little decay (76.8% of jams had a decay class of 2, and 16.0% had a decay class of 3), and decay rates in the Colorado semiarid mountains are slow compared to other environments (Kueppers et al., 2004). This indicates that the large amount of organic carbon in LW may remain an important carbon stock in West Creek over long time periods, although the ability for LW to remobilize off the floodplain and the flood magnitude required for remobilization have not been studied.

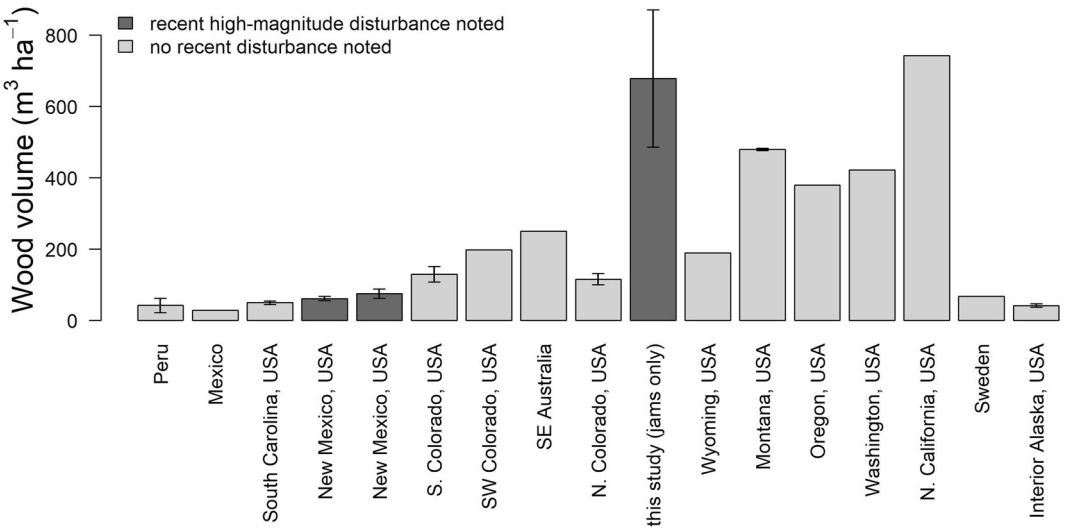

Figure 8. Comparison plot showing published average floodplain LW load across different environments, with bars representing averaged and whiskers showing plus or minus one standard error when available. Darker gray bars denote studies indicating that a high-magnitude disturbance had recently occurred. Plot shows data from Peru (Chao et al., 2008), Mexico (Jaramillo et al., 2003), South Carolina (Wohl et al., 2011), New Mexico (Wohl et al., 2018a), New Mexico (Wohl et al., 2018a), S. Colorado (Wohl et al., 2018a), SW Colorado (Wohl, 2020), SE Australia (Mac Nally et al., 2001), N. Colorado (Lininger et al., 2017), N. Colorado (this study), Wyoming (Wohl, 2020), Montana (Wohl et al., 2018b), Oregon (Nakamura & Swanson, 1994), Washington (Scott & Wohl, 2018), N. California (Busing & Fujimori, 2005), Sweden (Dahlström & Nilsson, 2006), and interior Alaska (Lininger et al., 2017). LW, large wood.

5. Conclusions

The bidirectional interactions between LW and CPOM, living vegetation, and geomorphic processes in river corridors have not been adequately explored, particularly in floodplains. LW has been used for restoration in river channels to enhance and create habitat for fish and other organisms, but management of floodplain LW is a new frontier. Because floodplain LW is likely less mobile than in-channel LW, floodplain LW used in restoration is likely less hazardous than in-channel LW but can provide ecological benefits and increase geomorphic complexity. In addition, geomorphologists have not adequately investigated the interactions between CPOM deposition and geomorphic characteristics.

Our main objective was to explore how river corridor morphology and forest stand characteristics influence the number and load of LW and CPOM jams in floodplains. We found that reaches with lower slopes contained larger loads of CPOM and LW, reaches with denser standing trees had more CPOM volume and jams per area, and LW jam size decreased with distance and elevation above the channel. Our results point to the important role of riparian forests in providing trapping locations for LW and CPOM on the floodplain and can inform river restoration efforts. However, further research is needed to determine the combined influence of geomorphic characteristics, flood events, and tree density and spatial variations on the formation and persistence of floodplain jams.

Data Availability Statement

Data are available in Supporting Information file and online at the University of Colorado Boulder Data Repository, which can be accessed at https://doi.org/10.25810/xgdx-5358.

Acknowledgments
We thank Anna Marshall and Alex Hurtado for field assistance, and Ellen Wohl for providing feedback on an early draft of the manuscript.

References

Barton, K. (2019). *MuMIn: Multi-Model Inference (version R package version 1.43.15)*. Retrieved from https://CRAN.R-project.org/package=MuMIn

Benke, A. C. (2011). Importance of flood regime to invertebrate habitat in an unregulated river–floodplain ecosystem. *Journal of the North American Benthological Society*, *20*(2), 225–240.

Bertoldi, W., Welber, M., Gurnell, A. M., Mao, L., Comiti, F., & Tal, M. (2015). Physical modelling of the combined effect of vegetation and wood on river morphology. *Geomorphology*, *246*, 178–187. https://doi.org/10.1016/j.geomorph.2015.05.038

Boos, M. F., & Boos, C. M. (1934). Granites of the front range—The Longs Peak-St. Vrain Batholith. *GSA Bulletin*, *45*(2), 303–332. https://doi.org/10.1130/GSAB-45-303

Braddock, W. A., & Cole, J. C. (1990). *Geologic Map of Rocky Mountain National Park and Vicinity, Colorado*. Denver, CO: US Geological Survey.

Braudrick, C. A., & Grant, G. E. (2001). Transport and deposition of large woody debris in streams: A flume experiment. *Geomorphology*, *41*(4), 263–283. https://doi.org/10.1016/S0169-555X(01)00058-7

Buechling, A., & Baker, W. L. (2004). A fire history from tree rings in a high-elevation forest of Rocky Mountain National Park. *Canadian Journal of Forest Research*, *34*, 1259–1273. https://doi.org/10.1139/x04-012

Busing, R. T., & Fujimori, T. (2005). Biomass, production and woody detritus in an old coast redwood (Sequoia sempervirens) forest. *Plant Ecology*, *177*(2), 177–188. https://doi.org/10.1007/s11258-005-2322-8

Bywater-Reyes, S., Wilcox, A. C., & Diehl, R. M. (2017). Multiscale influence of woody riparian vegetation on fluvial topography quantified with ground-based and airborne lidar: Woody Vegetation and Fluvial Topography. *Journal of Geophysical Research: Earth Surface*, *122*, 1218–1235. https://doi.org/10.1002/2016JF004058

Capesius, J. P., & Stephens, V. C. (2009). *Regional regression equations for estimation of natural streamflow statistics in Colorado*. U.S. Geological Survey.

Cenderelli, D. A., & Wohl, E. E. (2003). Flow hydraulics and geomorphic effects of glacial-lake outburst floods in the Mount Everest region, Nepal. *Earth Surface Processes and Landforms*, *28*(4), 385–407. https://doi.org/10.1002/esp.448

Chao, K.-J., Phillips, O. L., & Baker, T. R. (2008). Wood density and stocks of coarse woody debris in a northwestern Amazonian landscape. *Canadian Journal of Forest Research*, *38*(4), 795–805. https://doi.org/10.1139/X07-163

Collins, B. D., Montgomery, D. R., Fetherston, K. L., & Abbe, T. B. (2012). The floodplain large-wood cycle hypothesis: A mechanism for the physical and biotic structuring of temperate forested alluvial valleys in the North Pacific coastal ecoregion. *Geomorphology*, *139–140*, 460–470. https://doi.org/10.1016/j.geomorph.2011.11.011

Comiti, F., Lucía, A., & Rickenmann, D. (2016). Large wood recruitment and transport during large floods: A review. *Geomorphology*, *269*, 23–39. https://doi.org/10.1016/j.geomorph.2016.06.016

Compton, R. R. (1985). *Geology in the field*. New York, NY: Wiley.

Corenblit, D., Steiger, J., Gurnell, A. M., Tabacchi, E., & Roques, L. (2009). Control of sediment dynamics by vegetation as a key function driving biogeomorphic succession within fluvial corridors. *Earth Surface Processes and Landforms*, *34*(13), 1790–1810. https://doi.org/10.1002/esp.1876

Dahlström, N., & Nilsson, C. (2006). The dynamics of coarse woody debris in boreal Swedish forests are similar between stream channels and adjacent riparian forests. *Canadian Journal of Forest Research*, *36*(5), 1139–1148. https://doi.org/10.1139/x06-015

Davenport, F. V., Herrera-Estrada, J. E., Burke, M., & Diffenbaugh, N. S. (2020). Flood size increases nonlinearly across the Western United States in response to lower snow-precipitation ratios. *Water Resources Research*, *56*, e2019WR025571. https://doi.org/10.1029/2019WR025571

Dixon, S. J., & Sear, D. A. (2014). The influence of geomorphology on large wood dynamics in a low gradient headwater stream. *Water Resources Research*, *50*, 9194–9210. https://doi.org/10.1002/2014WR015947

Galia, T., Macurová, T., Vardakas, L., Škarpich, V., Matušková, T., & Kalogianni, E. (2020). Drivers of variability in large wood loads along the fluvial continuum of a Mediterranean intermittent river. *Earth Surface Processes and Landforms*, *45*(9), 2048–2062. https://doi.org/10.1002/esp.4865

Gurnell, A. (2007). Analogies between mineral sediment and vegetative particle dynamics in fluvial systems. *Geomorphology*, *89*(1), 9–22. https://doi.org/10.1016/j.geomorph.2006.07.012

Gurnell, A. (2014). Plants as river system engineers. *Earth Surface Processes and Landforms*, *39*(1), 4–25. https://doi.org/10.1002/esp.3397

Gurnell, A., & Petts, G. E. (2002). Island-dominated landscapes of large floodplain rivers: A European perspective. *Freshwater Biology*, *47*(4), 581–600. https://doi.org/10.1046/j.1365-2427.2002.00923.x

Harmon, M. E., Woodall, C. W., Fasth, B., Sexton, J., & Yatkov, M. (2011). Differences between standing and downed dead tree wood density reduction factors: A comparison across decay classes and tree species. In Res. Pap. NRS-15 (Vol. 40, pp. 1–40). Newtown Square, PA: U.S. Department of Agriculture, Forest Service, Northern Research Station. https://doi.org/10.2737/NRS-RP-15

Harvey, J., & Gooseff, M. (2015). River corridor science: Hydrologic exchange and ecological consequences from bedforms to basins. *Water Resources Research*, *51*, 6893–6922. https://doi.org/10.1002/2015WR017617

He, Q., & Walling, D. E. (1998). An investigation of the spatial variability of the grain size composition of floodplain sediments. *Hydrological Processes*, *12*(7), 1079–1094. https://doi.org/10.1002/(SICI)1099-1085(19980615)12:7<1079::AID-HYP642>3.0.CO;2-E

Hurvich, C., & Tsai, C. (1989). Regression and time series model selection in small samples. *Biometrika*, *76*, 291–307. https://doi.org/10.1093/biomet/76.2.297

Iroumé, A., Ruiz-Villanueva, V., Mao, L., Barrientos, G., Stoffel, M., & Vergara, G. (2018). Geomorphic and stream flow influences on large wood dynamics and displacement lengths in high gradient mountain streams (Chile). *Hydrological Processes*, *32*(17), 2636–2653. https://doi.org/10.1002/hyp.13157

Jaramillo, V. J., Kauffman, J. B., Rentería-Rodríguez, L., Cummings, D. L., & Ellingson, L. J. (2003). Biomass, carbon, and nitrogen pools in Mexican tropical dry forest landscapes. *Ecosystems*, *6*(7), 609–629. https://doi.org/10.1007/s10021-002-0195-4

Jeffries, R., Darby, S. E., & Sear, D. A. (2003). The influence of vegetation and organic debris on flood-plain sediment dynamics: Case study of a low-order stream in the New Forest, England. *Geomorphology*, *51*(1–3), 61–80. https://doi.org/10.1016/S0169-555X(02)00325-2

Jones, K. K., Anlauf-Dunn, K., Jacobsen, P. S., Strickland, M., Tennant, L., & Tippery, S. E. (2014). Effectiveness of instream wood treatments to restore stream complexity and winter rearing habitat for juvenile coho salmon. *Transactions of the American Fisheries Society*, *143*(2), 334–345. https://doi.org/10.1080/00028487.2013.852623

Jones, W. D., & Quam, L. O. (1944). Glacial land forms in rocky mountain national park, Colorado. *The Journal of Geology*, *52*(4), 217–234. https://doi.org/10.1086/625213

Krueger, J. I., & Heck, P. R. (2019). Putting the p-value in its place. *The American Statistician*, *73*(Suppl. 1), 122–128. https://doi.org/10.1080/00031305.2018.1470033

Kueppers, L. M., Southon, J., Baer, P., & Harte, J. (2004). Dead wood biomass and turnover time, measured by radiocarbon, along a subalpine elevation gradient. *Oecologia*, *141*(4), 641–651. https://doi.org/10.1007/s00442-004-1689-x

Kui, L., Stella, J. C., Lightbody, A., & Wilcox, A. C. (2014). Ecogeomorphic feedbacks and flood loss of riparian tree seedlings in meandering channel experiments. *Water Resources Research*, *50*, 9366–9384. https://doi.org/10.1002/2014WR015719

Lininger, K. B., & Latrubesse, E. M. (2016). Flooding hydrology and peak discharge attenuation along the middle Araguaia River in central Brazil. *CATENA*, *143*, 90–101. https://doi.org/10.1016/j.catena.2016.03.043

Lininger, K. B., & Scott, D. N. (2019). The role of floodplain wood in enhancing river corridor resilience. In *Oral presentation H51C-07 presented at the American Geophysical Union Fall Meeting*, San Francisco, CA.

Lininger, K. B., Wohl, E., Sutfin, N. A., & Rose, J. R. (2017). Floodplain downed wood volumes: A comparison across three biomes. *Earth Surface Processes and Landforms*, *42*(8), 1248–1261. https://doi.org/10.1002/esp.4072

Livers, B., Lininger, K. B., Kramer, N., & Sendrowski, A. (2020). Porosity problems: Comparing and reviewing methods for estimating porosity and volume of wood jams in the field. *Earth Surface Processes and Landforms*, *45*(13), 3336–3353. https://doi.org/10.1002/esp.4969

Mac Nally, R., Parkinson, A., Horrocks, G., Conole, L., & Tzaros, C. (2001). Relationships between terrestrial vertebrate diversity, abundance and availability of coarse woody debris on south-eastern Australian floodplains. *Biological Conservation*, *99*(2), 191–205. https://doi.org/10.1016/S0006-3207(00)00180-4

Manners, R. B., Doyle, M. W., & Small, M. J. (2007). Structure and hydraulics of natural woody debris jams. *Water Resources Research*, *43*, W06432. https://doi.org/10.1029/2006WR004910

Montgomery, D. R., & Abbe, T. B. (2006). Influence of logjam-formed hard points on the formation of valley-bottom landforms in an old-growth forest valley, Queets River, Washington, USA. *Quaternary Research*, *65*(1), 147–155. https://doi.org/10.1016/j.yqres.2005.10.003

Montgomery, D. R., Collins, B. D., Buffington, J. M., & Abbe, T. B. (2003). Geomorphic effects of wood in rivers. In S. V. Gregory, K. L. Boyer, & A. M. Gurnell (Eds.), *The ecology and management of wood in world rivers. American Fisheries Society Symposium* (Vol. 37, pp. 21–47). Retrieved from http://www.treesearch.fs.fed.us/pubs/23945

Nakamura, F., & Swanson, F. J. (1994). Distribution of coarse woody debris in a mountain stream, western Cascade Range, Oregon. *Canadian Journal of Forest Research*, *24*, 2395–2403. https://doi.org/10.1139/x94-309

Pettit, N. E., & Naiman, R. J. (2006). Flood-deposited wood creates regeneration niches for riparian vegetation on a semi-arid South African river. *Journal of Vegetation Science*, *17*(5), 615–624. https://doi.org/10.1111/j.1654-1103.2006.tb02485.x

Pettit, N. E., Naiman, R. J., Rogers, K. H., & Little, J. E. (2005). Post-flooding distribution and characteristics of large woody debris piles along the semi-arid Sabie River, South Africa. *River Research and Applications*, *21*(1), 27–38. https://doi.org/10.1002/rra.812

Pizzuto, J. E. (1987). Sediment diffusion during overbank flows. *Sedimentology*, *34*(2), 301–317. https://doi.org/10.1111/j.1365-3091.1987.tb00779.x

Ricker, M. C., Lockaby, B. G., Blosser, G. D., & Conner, W. H. (2016). Rapid wood decay and nutrient mineralization in an old-growth bottomland hardwood forest. *Biogeochemistry*, *127*, 1–338. https://doi.org/10.1007/s10533-016-0183-y

Roni, P., Beechie, T., Pess, G., & Hanson, K. (2015). Wood placement in river restoration: Fact, fiction, and future direction. *Canadian Journal of Fisheries and Aquatic Sciences*, *72*(3), 466–478. https://doi.org/10.1139/cjfas-2014-0344

Ruiz-Villanueva, V., Mazzorana, B., Bladé, E., Bürkli, L., Iribarren-Anacona, P., Mao, L., et al. (2019). Characterization of wood-laden flows in rivers: Wood-laden flows. *Earth Surface Processes and Landforms*, *44*(9), 1694–1709. https://doi.org/10.1002/esp.4603

Scott, D. N., & Wohl, E. (2018). Natural and anthropogenic controls on wood loads in river corridors of the rocky, cascade, and Olympic mountains, USA. *Water Resources Research*, *54*, 7893–7909. https://doi.org/10.1029/2018WR022754

Scott, D. N., Wohl, E., & Yochum, S. E. (2019). Wood Jam Dynamics Database and Assessment Model (WooDDAM): A framework to measure and understand wood jam characteristics and dynamics. *River Research and Applications*, *35*, 1466–1477. https://doi.org/10.1002/rra.3481

Sear, D. A., Millington, C. E., Kitts, D. R., & Jeffries, R. (2010). Logjam controls on channel: Floodplain interactions in wooded catchments and their role in the formation of multi-channel patterns. *Geomorphology*, *116*(3–4), 305–319. https://doi.org/10.1016/j.geomorph.2009.11.022

Sholtes, J. S., Yochum, S. E., Scott, J. A., & Bledsoe, B. P. (2018). Longitudinal variability of geomorphic response to floods. *Earth Surface Processes and Landforms*, *43*(15), 3099–3113. https://doi.org/10.1002/esp.4472

Sibold, J. S., Veblen, T. T., & González, M. E. (2006). Spatial and temporal variation in historic fire regimes in subalpine forests across the Colorado Front Range in Rocky Mountain National Park, Colorado, USA. *Journal of Biogeography*, *33*(4), 631–647. https://doi.org/10.1111/j.1365-2699.2005.01404.x

Smith, H. G., Sheridan, G. J., Lane, P. N. J., Nyman, P., & Haydon, S. (2011). Wildfire effects on water quality in forest catchments: A review with implications for water supply. *Journal of Hydrology*, *396*(1), 170–192. https://doi.org/10.1016/j.jhydrol.2010.10.043

Steeb, N., Rickenmann, D., Badoux, A., Rickli, C., & Waldner, P. (2017). Large wood recruitment processes and transported volumes in Swiss mountain streams during the extreme flood of August 2005. *Geomorphology*, *279*, 112–127. https://doi.org/10.1016/j.geomorph.2016.10.011

Thompson, C. G., Kim, R. S., Aloe, A. M., & Becker, B. J. (2017). Extracting the variance inflation factor and other multicollinearity diagnostics from typical regression results. *Basic and Applied Social Psychology*, *39*(2), 81–90. https://doi.org/10.1080/01973533.2016.1277529

Veblen, T. T., & Donnegan, J. A. (2005). *Historical range of variability for forest vegetation of the national forests of the Colorado Front Range*. USDA Forest Service, Rocky Mountain Region. Retrieved from http://coloradoforestrestoration.org/wp-content/uploads/2014/11/2005_HRVFrontRangeForests.pdf

Wagenmakers, E.-J., & Farrell, S. (2004). AIC model selection using Akaike weights. *Psychonomic Bulletin and Review*, *11*(1), 192–196. https://doi.org/10.3758/BF03206482

Wohl, E. (2020). Wood process domains and wood loads on floodplains. *Earth Surface Processes and Landforms*, *45*(1), 144–156. https://doi.org/10.1002/esp.4771

Wohl, E., Bledsoe, B. P., Fausch, K. D., Kramer, N., Bestgen, K. R., & Gooseff, M. N. (2016). Management of large wood in streams: An overview and proposed framework for hazard evaluation. *JAWRA Journal of the American Water Resources Association*, *52*(2), 315–335. https://doi.org/10.1111/1752-1688.12388

Wohl, E., Cadol, D., Pfeiffer, A., Jackson, K., & Laurel, D. (2018). Distribution of large wood within river corridors in relation to flow regime in the semiarid western US. *Water Resources Research*, *54*, 1890–1904. https://doi.org/10.1002/2017WR022009

Wohl, E., & Goode, J. R. (2008). Wood dynamics in headwater streams of the Colorado Rocky Mountains: Wood dynamics in Colorado. *Water Resources Research*, *44*, W09429. https://doi.org/10.1029/2007WR006522

Wohl, E., Hinshaw, S. K., Scamardo, J. E., & Gutiérrez-Fonseca, P. E. (2019). Transient organic jams in Puerto Rican mountain streams after hurricanes. *River Research and Applications*, *35*, 280–289. https://doi.org/10.1002/rra.3405

Wohl, E., Polvi, L. E., & Cadol, D. (2011). Wood distribution along streams draining old-growth floodplain forests in Congaree National Park, South Carolina, USA. *Geomorphology*, *126*(1–2), 108–120. https://doi.org/10.1016/j.geomorph.2010.10.035

Wohl, E., Scott, D. N., & Lininger, K. B. (2018). Spatial distribution of channel and floodplain large wood in forested river corridors of the Northern Rockies. *Water Resources Research*, *54*, 7879–7892. https://doi.org/10.1029/2018WR022750

Woltemade, C. J., & Potter, K. W. (1994). A watershed modeling analysis of fluvial geomorphologic influences on flood peak attenuation. *Water Resources Research*, *30*, 1933–1942. https://doi.org/10.1029/94WR00323

Yochum, S. E., & Collins, F. (2015). Colorado Front Range Flood of 2013: Peak flows and flood frequencies. In *Paper presented at Proceedings of the 3rd Joint Federal Interagency Conference on Sedimentation and Hydrologic Modeling* (p. 12), Reno, Nevada, USA.

Yochum, S. E., & Moore, D. S. (2013). *Colorado Front Range flood of 2013: Peak flow estimates at selected mountain stream locations (Technical Report, p. 44)*. USDA Natural Resources Conservation Service.

Zalamea, M., González, G., Ping, C.-L., & Michaelson, G. (2007). Soil organic matter dynamics under decaying wood in a subtropical wet forest: Effect of tree species and decay stage. *Plant and Soil*, *296*(1–2), 173–185. https://doi.org/10.1007/s11104-007-9307-4

Zischg, A. P., Galatioto, N., Deplazes, S., Weingartner, R., & Mazzorana, B. (2018). Modelling spatiotemporal dynamics of large wood recruitment, transport, and deposition at the river reach scale during extreme floods. *Water*, *10*(9), 1134. https://doi.org/10.3390/w10091134